MICROSTRUCTURAL AND TRIBOLOGICAL PROPERTIES OF NICKEL-BASED HARDFACING COATINGS APPLIED ON NITRIDING STEELS BY PLASMA TRANSFERRED ARC WELDING

Gökçe Mehmet AY[1*], Fatih Hayati ÇAKIR[2], Abdullah SERT[3]

[1*] Eskişehir Osmangazi Üniversitesi Makine Mühendisliği Bölümü, Eskişehir.
ORCID No: https://orcid.org/0000-0001-8354-5070
[2] Eskişehir Osmangazi Üniversitesi, Eskişehir Meslek Yüksek Okulu, Eskişehir,
ORCID No: https://orcid.org/ 0000-0002-0873-5920
[3] Eskişehir Osmangazi Üniversitesi Makine Mühendisliği Bölümü, Eskişehir.
ORCID No: https://orcid.org/ 0000-0002-2406-0409

Keywords

Surface Modification, Plasma Transferred Arc, Boron Carbide

Abstract

Plasma Transferred Arc (PTA) coatings are widely used for the surface modification of metals due to their ability to achieve high coating thickness, low thermal stress, and high energy density. This technique is commonly applied to glass and ceramic molds, automotive valves, petrochemical vanes, lamination cylinders, as well as plastic extrusion molds and screws. In plastic injection machine screws, high hardness and wear resistance are essential for durability. To achieve these properties, the steels used in plastic injection screws are first hardfaced on the thread crests using the PTA coating method and then nitrided. In this study, 1.8550 and 1.8519 steels, commonly used in plastic injection screw manufacturing, were coated with two different powders: FeCrBSi with a nickel (Ni) balance, either with or without tungsten (W) addition. The tribological properties of the coated samples were evaluated through ball-on-disc wear tests. The samples were characterized using X-ray diffraction (XRD), scanning electron microscopy (SEM), energy-dispersive spectroscopy (EDS), and optical microscopy. The depth and width of wear tracks were measured using a profilometer. Results indicated that increasing W content leads to a higher coefficient of friction, but the best wear performance was observed with W-containing coatings. The optimal combination was found to be the 1.8550 steel substrate paired with the FeCrBSi-W coating, which demonstrated a 5% higher coefficient of friction but a 47% lower specific wear rate compared to the non-W coating.

PLAZMA TRANSFER ARK KAYNAĞI İLE NİTRÜRLENMİŞ ÇELİKLER ÜZERİNE KAPLANMIŞ NİKEL ESASLI SERT DOLGU KAPLAMALARININ MİKROYAPISAL VE TRİBOLOJİK ÖZELLİKLER

Anahtar Kelimeler

Yüzey geliştirme, Plazma transfer ark, Bor karbür

Öz

Plazma Transfer Ark (PTA) kaplamaları, yüksek kaplama kalınlığı, düşük termal gerilim ve yüksek enerji yoğunluğu sağladıkları için metallerin yüzey modifikasyonunda yaygın olarak kullanılmaktadır. Bu teknik, cam ve seramik kalıplar, otomotiv valfleri, petrokimyasal kanatlar, lamine silindirler ve plastik ekstrüzyon kalıpları ve vidalarına uygulanmaktadır. Plastik enjeksiyon makinesi vidalarında yüksek sertlik ve aşınma direnci, dayanıklılık için kritik öneme sahiptir. Bu özelliklerin elde edilmesi için plastik enjeksiyon vidalarında kullanılan çeliklerin diş tepeleri önce PTA yöntemiyle sert dolgu kaplama ile kaplanır, ardından nitrürleme işlemi uygulanır. Bu çalışmada, plastik enjeksiyon vidaları üretiminde kullanılan 1.8550 ve 1.8519 çelikleri, nikel (Ni) esaslı ve tungsten (W) katkılı veya katkısız FeCrBSi tozları ile kaplanmıştır. Kaplanmış numunelerin tribolojik özellikleri bilye-disk aşınma testleriyle değerlendirilmiştir. Numuneler, X-ışını difraksiyonu (XRD), taramalı elektron mikroskobu (SEM), enerji dağılımlı spektroskopi (EDS) ve optik mikroskop analizleri ile karakterize edilmiştir. Aşınma izlerinin derinliği ve genişliği bir profilometre kullanılarak ölçülmüştür.Sonuçlar, artan W içeriğinin sürtünme katsayısını artırdığını, ancak en iyi aşınma performansının W içeren kaplamalarla elde edildiğini göstermiştir. En uygun kombinasyon, %5 daha yüksek sürtünme katsayısına rağmen %47 daha düşük spesifik aşınma oranı gösteren FeCrBSi-W kaplamalı 1.8550 çelik altlık olmuştur.

Araştırma Makalesi
Başvuru Tarihi : 13.09.2024
Kabul Tarihi : 21.04.2025

Research Article
Submission Date : 13.09.2024
Accepted Date : 21.04.2025

* Sorumlu yazar: gma@ogu.edu.tr
https://doi.org/10.31796/ogummf.1547071

1. Introduction

Many engineering applications require materials with high strength, as well as corrosion and wear resistance. In industry, steel is widely used for most applications, but its properties may not be sufficient for some specialized needs. In such cases, enhancing the surface of the material can provide significant benefits, and various surface modification techniques are employed. One such technique is Plasma Transferred Arc (PTA) coating. PTA coating is a surface modification method that uses a plasma arc to melt both the substrate and the coating material, creating a metallurgically bonded layer with improved surface properties. The literature contains a variety of studies focusing on the application of PTA coatings to enhance the wear resistance, hardness, and corrosion resistance of different substrates. These studies demonstrate that PTA coatings can be customized by adjusting process parameters, such as arc current and powder composition, to achieve desired microstructural characteristics and mechanical properties. For instance, lower arc currents have been associated with refined microstructures and improved hardness and corrosion resistance (Appiah et al., 2024). Incorporating different carbides, such as WC, NbC, and TiC, into the coatings has been shown to significantly enhance wear resistance (Appiah et al. 2022; Chen and Lin 2024; Das and Kumar 2024). Additionally, the shape of carbide particles, whether spherical or angular, influences the hardness and wear resistance of the coatings (ArunKumar, Prakash and Deenadayalan, 2023; Zhou et al., 2023). The addition of elements like vanadium, chromium, and nitrogen has also been reported to contribute to the formation of hard precipitates and improved coating performance (Guo, Zhang and Wang, 2023; Li et al., 2023). PTA coating is a versatile process that can be optimized to produce coatings with superior surface properties for various industrial applications (López et al., 2023). On steel parts, coatings with base materials such as Nickel, Cobalt, Stainless Steel, or Alloy Steels are commonly used, often with the addition of carbides like WC, Cr_2C_3, TiC, VC, NbC, and SiC. The PTA technique, with its capability for very high coating thicknesses, reduced thermal stress on the material, and high energy density, is used in various industries including glass and ceramic molds, automotive valves, petrochemical vanes, lamination cylinders, and plastic extrusion molds and screws (Hirpara, Valaki, Chaudhari and Siddhpura, 2024; Kishore, Jaiswal, Prabhakaran and Arora, 2023).

2. Literature Review

Steels used in plastic molds and screws require high hardness and wear resistance to ensure product longevity (Berins, 2012). To achieve these properties, surface hardening methods such as nitriding are employed. The most commonly used steels are 1.8550 (34CrAlNi7-10) and 1.8519 (31CrMoV9). The high aluminum content in 1.8550 results in surface hardness of 1000 HV after nitriding, but the low toughness of this layer limits its applications. Therefore, aluminum-free steels, such as 1.8519 or 1.7735 (14CrMoV6-9), are preferred (Mennig and Stoeckhert, 2013).

When examining the wear mechanisms in the plastic mold industry, galling and adhesion are identified as the prominent issues. These mechanisms are exacerbated by high-temperature corrosion and abrasive wear. To prevent further degradation, coatings that offer corrosion and abrasion resistance at elevated temperatures (around 200°C) are required. Among the available options, nickel-based coatings show promise for their corrosion and high-temperature resistance, though their abrasion resistance is somewhat limited.

In certain applications, alloying elements are added to the coating powders to enhance the abrasion resistance of the coatings. One advantage of using hardfacing, rather than thin-film coatings, is that worn surfaces can be repaired and reused. Plasma Transferred Arc (PTA) is a technique capable of applying coatings with substantial thickness. With the aid of numerical control, PTA coatings can be applied repeatedly to parts with various geometries, ensuring precise surface coverage.

PTA coating on plastic molds and screws presents an interesting opportunity for manufacturing. Since PTA coating can be applied selectively to areas of parts that are more prone to wear, it can significantly extend part life. Nickel-based (Ni-based) alloys have demonstrated excellent corrosion resistance (Maros and Siddiqui, 2022), and the addition of carbides to the powder increases wear resistance. Furthermore, as surface hardness increases, contact fatigue resistance also improves.

In this study, two different steels 1.8519 and 1.8550, commonly used in the plastic injection industry were coated using the PTA technique. The coating powders employed were commercial PTA powders (Colmonoy 56 and Colmonoy 57). Although these coating powders have been studied separately, the combination of these

specific powders with these steels has not been previously examined in the literature. Cross-sections of the coated surfaces were taken and analyzed using an optical microscope, confirming that the coating process was successful without any significant issues. Hardness and microstructure analyses were also conducted.

The tribological properties of the samples were investigated using a Ball-on-Disc test, and the coefficient of friction and specific wear rates were measured.

3. Method

3.1. Materials and welding parameters

Two commercially available PTA coating powders and two different steel specimens were used in the PTA process. The chemical compositions of the coating powders and steel specimens are provided in Tables 1 and 2, respectively.

Table 1. Composition of Powders Used for PTA in wt%

Powder	Bal	C	Cr	B	Si	Fe	W
Colmonoy 56 (C56)	Ni	0.9	18	1.9	5.3	5.4	-
Colmonoy 57 (C57)	Ni	0.5	11.5	2.5	3.5	3.5	16

Table 2. Compositions of Steels in wt%

Steel	C	Si	Mn	Ni
1.8519	0.27-0.34	0.4	0.4-0.7	-
	Cr	Mo	V	Al
	2.3-2.7	0.15-0.25	0.1-0.2	-
1.8550	C	Si	Mn	Ni
	0.3-0.37	max 0.4	0.4-0.7	0.85-1.15
	Cr	Mo	V	Al
	1.5-1.8	0.15-0.25	-	0.8-1.2

The substrates dimensions were machined to 100 × 42 × 20 mm. A canal of 10 mm width and 4 mm depth were machined to facilitate coating powders. Coating was performed using an automated Stellite Coating Star III (see Figure 1). The selection of welding parameters for the PTA process was aimed at achieving thick, pore-free coatings. The current was set to 100-105 A to ensure uniform heating of the workpiece, promoting consistent bonding and repeatable powder penetration. The PTA process was conducted in two passes to enhance the coating quality. The shielding gas flow rate was maintained at 12 L/min, the feed gas flow rate at 3 L/min, and the powder feed rate at 100 g/min. To further optimize the coating process, the substrates were preheated to 350°C before the PTA process and were allowed to cool in air after coating. The parameter tuning process was also carried out in collaboration with Enformak Company to refine the process and ensure reproducibility.

The primary objective of using PTA coating in this study is to produce crack- and pore-free thick coatings. To achieve this, powders with high nickel content, as nickel is well-known for its excellent wetting capabilities and ability to compensate for thermal differences, thus preventing cracks. The matrix of the coating is predominantly formed by nickel, which promotes good wetting of the molten powder onto the substrate and contributes to the formation of a hard surface to enhance wear resistance. Additionally, plastic injection molds often experience adhesive wear, where hot, molten plastic can adhere both chemically and mechanically to the mold surface. The selected powders, Colmonoy 56 and 57, are known for their durability in such conditions, making them ideal choices for enhancing the wear and adhesive resistance of the mold substrates, 1.8519 and 1.8550, which are commonly used in industrial applications.

Figure 1. Stellite Coating Star III PTA Machine

Table 3. Sample Coating and Substrate

Steel	Coating Powder	Sample No
1.8519	Colmonoy 56	A1
1.8519	Colmonoy 57	A2
1.8550	Colmonoy 56	B1
1.8550	Colmonoy 57	B2

This study complies with research and publication ethics.

3.2. Microstructure

To reveal the microstructure, coating samples were taken and prepared for metallographic analysis. The polished samples were etched using Murakami's reagent (ASM International et al., 2000) at 25°C for 60 seconds, and optical inspection was conducted with a Nikon Eclipse L150 optical microscope. Subsequently, samples were examined using a JEOL JSM 5600LV Scanning Electron Microscope and analyzed with a Panalytical Empyrian X-ray Diffractometer (XRD).

3.3. Microhardness and Wear Properties

Microhardness values were measured using a Vickers hardness tester with a 100 g load and a 10-second dwell time, with measurements taken 500 µm apart within the coating area. Another set of samples was prepared for wear tests. These samples were mounted, and their surfaces were ground. Surface roughness was measured before the wear tests using a Mitutoyo SJ 400 surface profilometer (see Hata! Başvuru kaynağı bulunamadı.a). It was confirmed that the surface roughness values of all samples were below 0.15 µm.

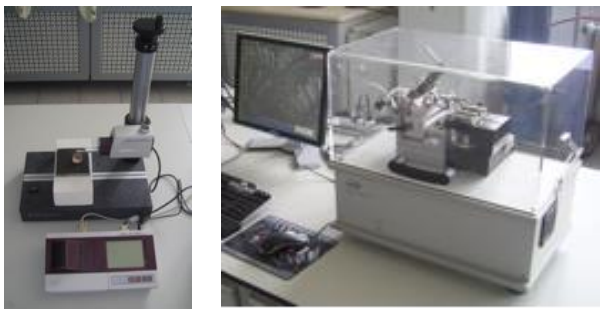

a) b)

Figure 2. Surface Roughness (a) Mitutoyo SJ 400) and Tribometer (b)CSM Ball-on-Disk Tribometer) Devices

A CSM Ball-on-Disk tribometer (see Figure 2b) was used for the wear tests. The samples were tested at a peripheral speed of 2.5 cm/s for a distance of 100 meters, under a 5 N load. The wear tests were conducted at room temperature (25°C) and 30%-35% humidity. For each test, a Si_3N_4 ball (E = 310 GPa, Hardness = 1580 kg/mm^2) with a diameter of 3 mm, certified for sphericity and composition by Red Hill Precision, was used as the counterpart. The Si_3N_4 ball was selected to ensure that no wear would occur on the ball itself. A schematic of the test setup is shown in Figure 3. SEM and EDS were used to examine the wear tracks. The sliding wear rates of the samples were calculated using data from the measured wear tracks, which was obtained with a surface roughness measurement instrument.

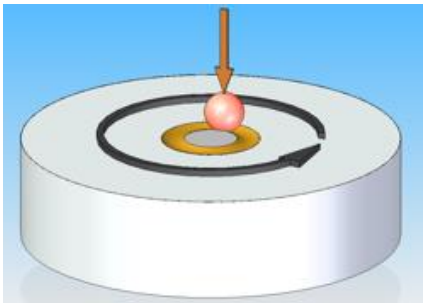

Figure 3. Schematic Drawing of Wear Geometry

4. Results and Discussion

4.1. Hardness

Coating hardness values were measured using Future Tech microhardness tester with 500µm intervals. Results were given in Figure 4.

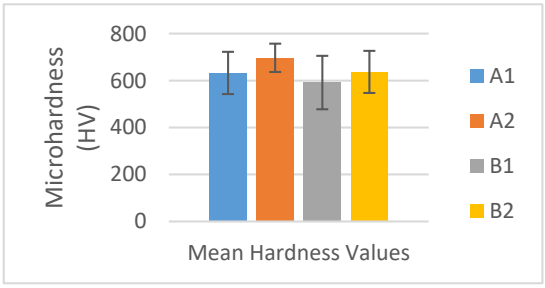

Figure 4. Hardness Values of Samples

4.2. Microstructure

Optical microscopy images of the samples reveal different phase formations in the microstructure. Figures 5a and 5b show the differentiation between the coating and the substrate. Upon inspection, it was found that the microstructures vary with changes in the coating powder, as illustrated in Figures 5a, 5c, and 5b, 5d. Closer examination of the samples reveals the presence of dendritic structures and dark carbide particles in the coating, as shown in Figures 5e, 5f, and 5g.

The samples were examined using scanning electron microscopy (SEM) along with energy dispersive spectroscopy (EDS) analysis, providing a detailed insight into their microstructural features. Cross-sectional images of the A1 and B1 samples reveal a pronounced dendritic growth of γNi, as clearly shown in Figures 6a and 6b (Sun, Tian, Ning Tian, Yu, and Meng, 2014). This dendritic pattern is indicative of the primary solidification process during alloy formation, suggesting rapid cooling and directional solidification which can affect the material's mechanical properties.

Additionally, the SEM images reveal floret-type chromium (Cr) microstructures, visible in Figures 6a, 6d, and 6g. These structures exhibit a characteristic pattern that has been previously reported in the literature (Kesavan and Kamaraj, 2010). The presence of these floret-like formations suggests localized segregation of Cr during solidification, which might influence the corrosion resistance and overall performance of the alloy.

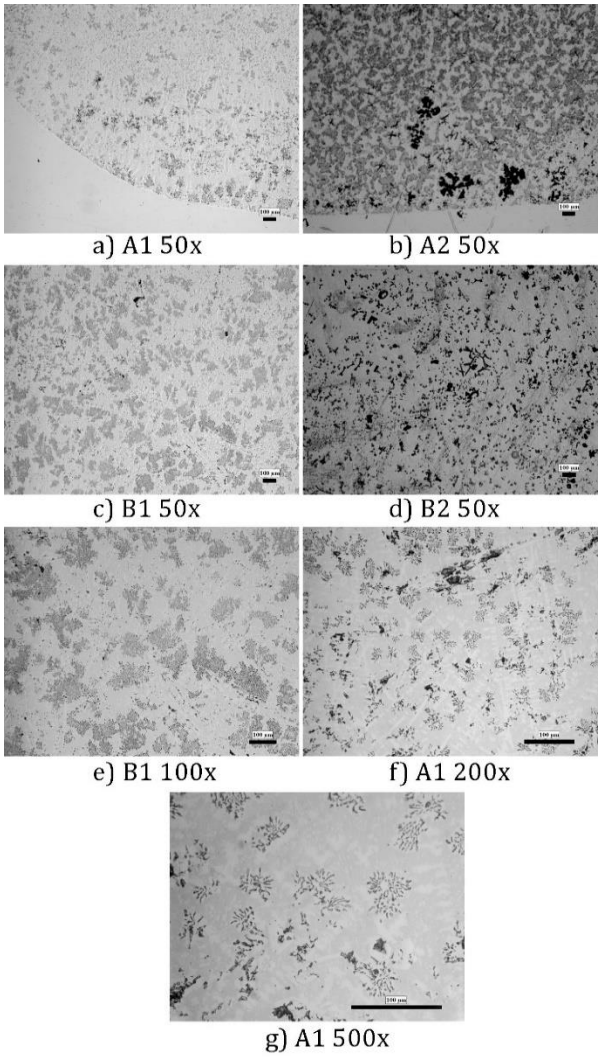

Figure 5. Microstructure of Samples

Furthermore, blocky carbide microstructures are observed in Figures 6d, 6e, 6f, and 6g. Detailed EDS analysis confirmed that these carbides are rich in chromium, thereby identifying them as chromium carbides (Hemmati, Rao, Ocelík and Hosson, 2013). The formation of these carbides is crucial, as they are known to contribute significantly to the hardness and wear resistance of the material by acting as reinforcing phases within the matrix.

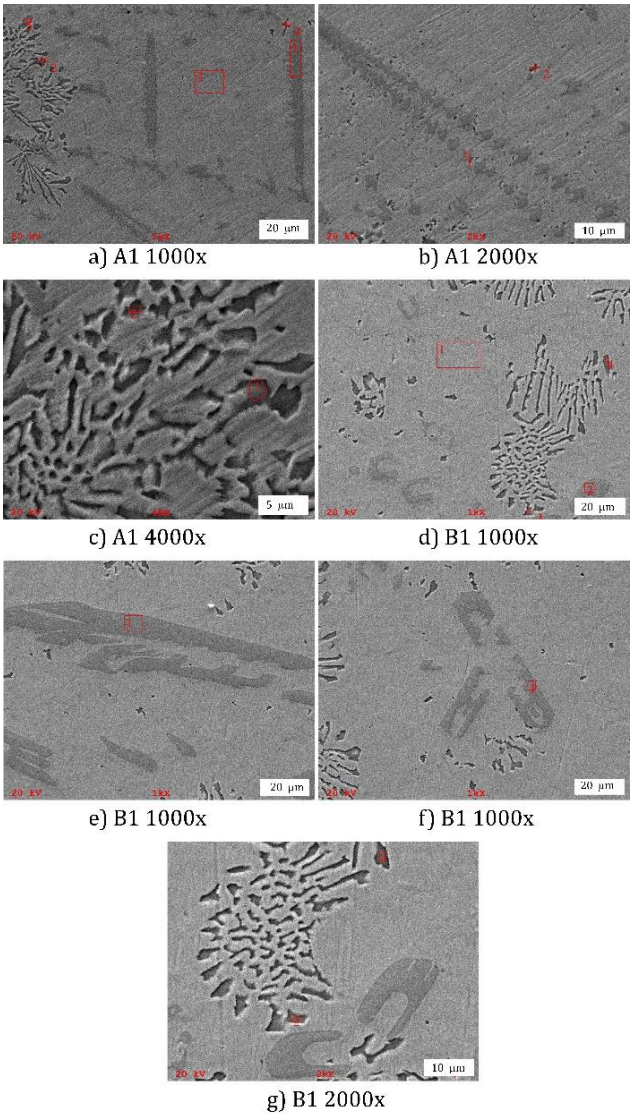

Figure 6. SEM Images of Samples A1 and B1

SEM images of the A2 and B2 samples reveal a complex distribution of carbide particles throughout the microstructure. In Figures 7a, 7d, and 7f, well-defined angular carbide particles are observed, indicating that these phases have formed with distinct boundaries. Their angular morphology suggests that these particles are likely to contribute significantly to the material's hardness and wear resistance by providing mechanical reinforcement within the matrix.

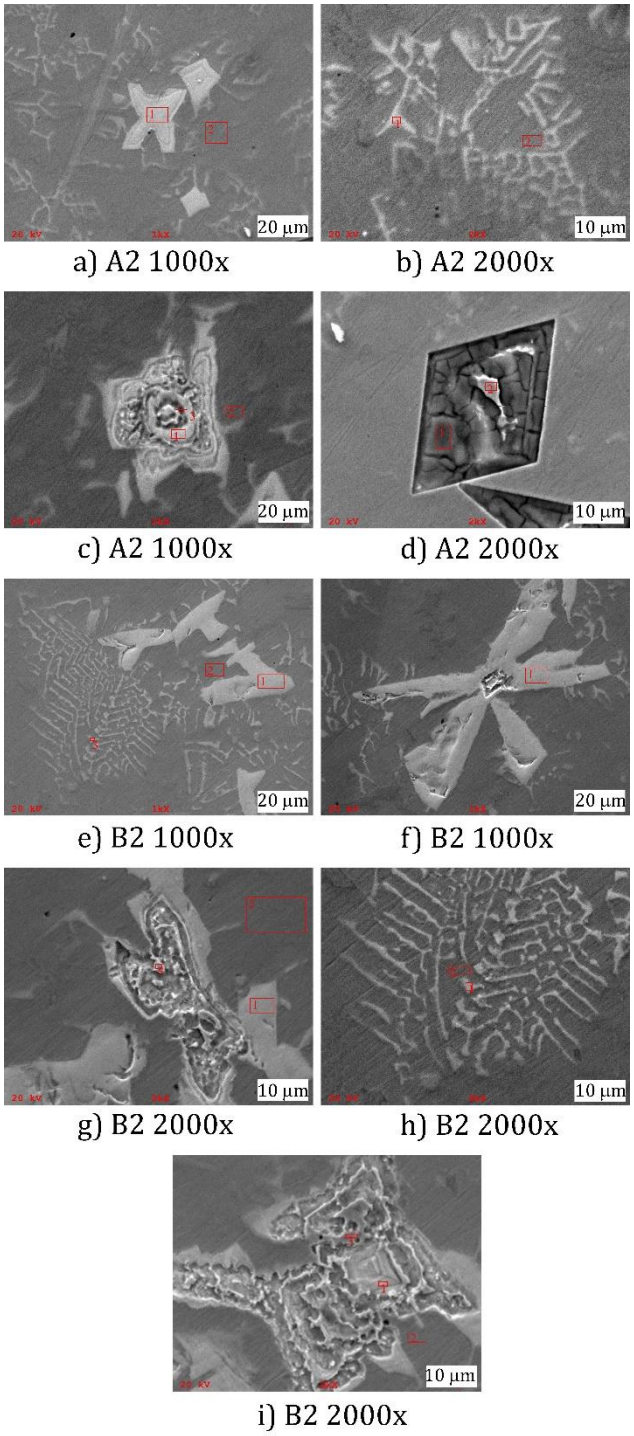

Figure 7. SEM Images of Samples A2 and B2

In contrast, Figures 7c, 7g, and 7i show deformed and dissipated angular particles. This variation in morphology may result from localized mechanical stresses or partial dissolution during wear, implying that these particles are subject to dynamic interactions within the material. EDS analysis of these regions revealed a higher tungsten (W) content, confirming that these are WC particles. The observation of WC particles at various dissolution levels is consistent with the findings reported by Lu and Kwon and Öteyaka, Arslan, and Çakir, suggesting that the processing conditions might be influencing the stability and integrity of these carbides (Lu and Kwon, 2002; Öteyaka, Arslan, and Çakir, 2021).

Additionally, Figures 7b, 7e, and 7h display M6C eutectic carbide structures. The presence of these microstructures is highlighted by their distinct morphology and composition, with EDS analysis indicating higher chromium content. This suggests that the M6C structures are likely chromium carbide microstructures, similar to those described in the literature (Ferreira et al., 2015). These carbides are typically formed during the eutectic solidification process, and their presence can have a pronounced effect on the alloy's overall wear behavior and mechanical performance.

4.3.XRD analysis

Figure 8 presents the XRD analysis of the A1, A2, B1, and B2 samples after coating. The XRD patterns are very similar across the four samples, with only minor differences. The types of elements in the powders used for the coatings are the same, except for the presence of W in Colmonoy 57. The differences in element percentages are provided in Table 1.

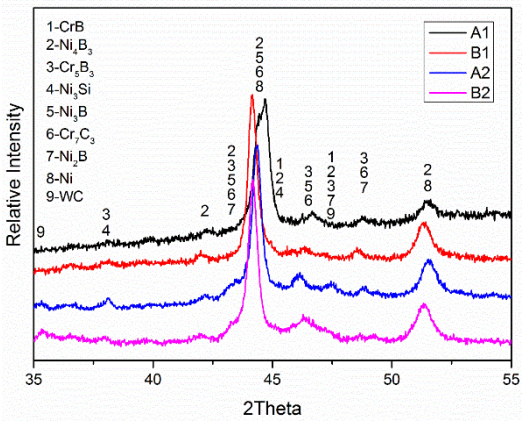

Figure 8. XRD Result of Samples

Examination of the XRD patterns reveals that the A2 and B2 coatings contain peaks corresponding to the W element, which constitutes 16% of the coating, unlike the A1 and B1 samples. The Ni content in the powders used for coating is 68.5% by weight in Colmonoy 56 and 62.5% by weight in Colmonoy 57. Due to the high Ni content, the Ni peaks obscure the detection of peaks from elements present in lower concentrations within the coating and substrate. The overlapping of peaks from different phases at the same diffraction angles complicates the determination of peak intensities. XRD diffraction identified peaks corresponding to carbide (Cr_7C_3, WC) and boride (CrB, Cr_5B_3, Ni_3B, Ni_4B_3, Ni_2B) phases associated with Ni and Cr elements. These phases align with results from similar coating studies as

reported in the literature (Hemmati et al., 2013; Silva and D'Oliveira, 2017; Yang et al., 2016). The presence of these phases was confirmed by SEM and EDS analyses.

4.4. Wear Test

Figures 9, 10, and 11 show the relationship between distance and the coefficient of friction (CoF), specific wear rate (SWR), and the average CoF obtained from wear tests, respectively. Upon close inspection, it was observed that changes in substrate and coating significantly affect both CoF and SWR. As expected, the coefficient of friction was influenced by the coating material, as illustrated in Figure 11. Colmonoy 57 was found to be the best coating material in terms of friction characteristics. The substrate type had a minimal effect on the friction characteristics of the sample, which aligns with expectations. For coatings where the coating thickness exceeds the substrate's surface roughness, the substrate has little impact on the friction coefficient (Kato, 2000). Since the total wear track depth was less than the coating thickness, the friction was primarily influenced by the coating material. The high friction coefficient observed in the A2 and B2 samples was attributed to the W content in Colmonoy 57. XRD results and SEM images indicated the presence of WC on the surface. These hard particles increase the run-in time, as shown in Figure 9. With increasing test distance, the removal of hard particles leads to a CoF peak. The softer Ni layer contributes to a higher CoF. In contrast, the higher Cr content in Colmonoy 56 results in dispersed CrB and CrC particles within the coating. These dispersed particles lead to a shorter run-in time and a lower CoF peak. Therefore, Colmonoy 56 exhibited better friction characteristics.

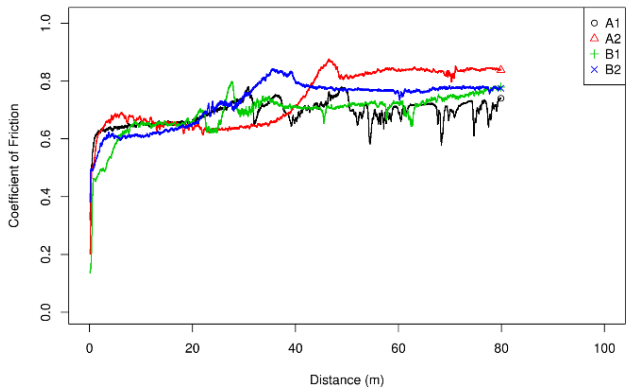

Figure 9. Friction Coefficient Versus Distance Graph

The results of the wear characteristics indicate that the substrate significantly affects the wear properties of the samples. Wear is a complex phenomenon influenced by various material and system properties. Figure 10 shows that steel 1.8550 (samples B1 and B2) exhibited less wear, regardless of the coating applied. Among these, sample B2, which was coated with a WC-containing powder, demonstrated the best wear performance. In contrast, sample A2, despite being coated with the same powder, exhibited the poorest wear behavior.

SEM images of the wear track on sample A2 (Figure 12c) clearly reveal a distinct layering on the worn surface. This layering likely results from the continuous deposition of wear debris during the sliding process. However, these layers are not stable; they exhibit noticeable cracking, which indicates that the bond between successive layers is weak. In Figure 12d, third-body particles formed due to wear are visible. These particles can act as abrasives, further contributing to the wear process by aggravating the removal of surface material.

The observed layering and subsequent layer removal in sample A2 correlate well with the Coefficient of Friction (CoF) versus Distance graph. For the initial 40 meters of sliding, the CoF remains stable, suggesting that the deposited layers temporarily protect the surface. After this point, the occurrence of layer cracking and removal exposes the substrate, resulting in an increased CoF as the frictional conditions change due to direct contact between the sample and the counterface.

In contrast, SEM images of the wear track for sample B2 (Figures 12e and 12f) demonstrate better layer adhesion. This implies that the wear debris on B2 forms a more continuous and robust tribolayer, which can effectively reduce the friction and protect the surface from further degradation.

Furthermore, SEM images for samples A1 and B1 (Figures 12a and 12b) show that both exhibit similar wear track structures and specific wear rates. Comparable morphology suggests that similar wear mechanisms are at play in these samples. Their similar specific wear rates—quantitative measures of material loss—indicate that the underlying microstructures and alloying effects lead to analogous tribological performance.

The overall reduced wear rate observed in steel 1.8550 is attributed to its higher nickel (Ni) and aluminum (Al) content (Takaki, Furuya and Tokunaga, 1990). These elements improve the toughness of the alloy, which enhances its ability to resist crack initiation and propagation within the protective layers. Consequently, this results in fewer instances of layer cracking and a more durable wear surface, which contributes to the lower wear rate.

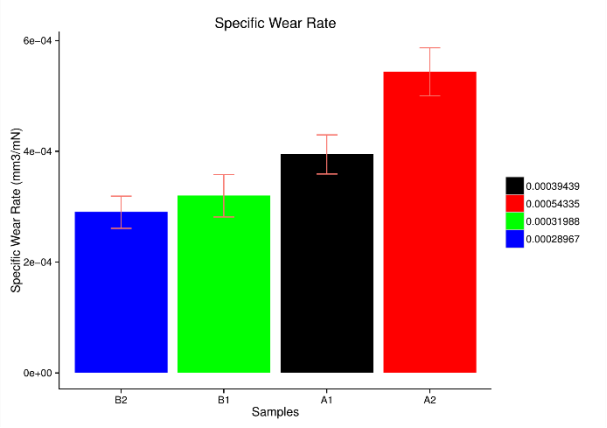

Figure 10. Specific Wear Rate of Samples

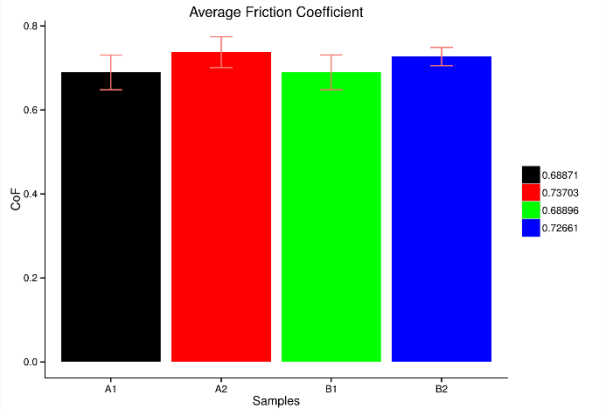

Figure 11. Average Coefficient of Friction of Samples

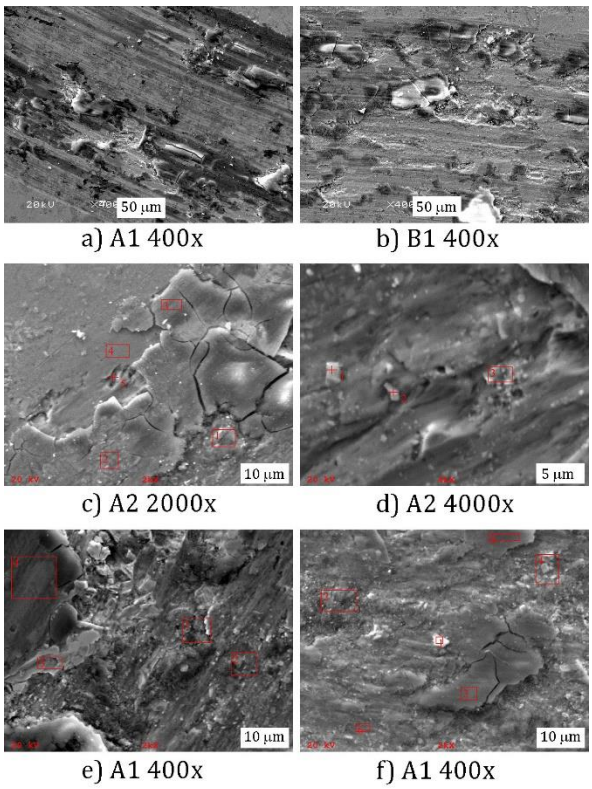

Figure 12. SEM Images of Wear Track Samples

5. Conclusions

PTA hardfacing coatings are crucial for enhancing the tribological properties of metals used in machine parts. Examining PTA coatings on nitriding steels assists designers in selecting high-performance coating materials and substrate pairs. This study investigated the friction and wear characteristics of two nitriding-class steels with two different coating powders. The following conclusions were reached:

- Lower friction is achieved with coating powders containing less tungsten (W). PTA coatings with higher hard particle content on the surface result in a higher coefficient of friction (CoF).
- Lower specific wear rates are dependent on the combination of substrate and coating powder. The best results were obtained with 1.8550 substrates and FeCrBSi coating powder containing higher W content.
- The optimum pair was identified as 1.8550 with FeCrBSi-W coating. This combination exhibits a 5% higher CoF but a 47% lower wear rate.

Araştırmacıların Katkısı

Gökçe Mehmet AY: Makale yazımı, kontrol ve triboloji testlerinin değerlendirilmesi

Fatih Hayati ÇAKIR: XRD analizleri ve değerlendirilmesi

Abdullah SERT: PTA ve sertlik testlerinin değerlendirilmesi

Çıkar Çatışması

Yazarlar tarafından herhangi bir çıkar çatışması beyan edilmemiştir.

Kaynaklar

Appiah, A. N. S., Oktawian, B., Marcin, Ż., Artur, C., David K. S., & Marcin A. (2022). Hardfacing of Mild Steel with Wear-Resistant Ni-Based Powders Containing Tungsten Carbide Particles Using Powder Plasma Transferred Arc Welding Technology. *Materials Science-Poland,* 40(3), 42–63. doi: 10.2478/msp-2022-0033.

Appiah, A. N. S., Bernard, W., Krzysztof, M., Łukasz, R., Oktawian, B., Gilmar, F. B., Artur, C., & Marcin, A. (2024). Microstructure and Performance of NiCrBSi Coatings Prepared by Modulated Arc Currents Using Powder Plasma Transferred Arc Welding Technology. *Applied Surface Science,* 648, 159065. doi: 10.1016/j.apsusc.2023.159065.

ArunKumar, V., Prakash, N., & Deenadayalan, K. (2023). Comparison between the Spherical and Angular Type WC Particles Reinforced in Nickel-Based Matrix Deposited Using Plasma Transferred Arc Welding Process. *Materials Today: Proceedings,* S2214785323009082. doi: 10.1016/j.matpr.2023.02.344.

ASM International, Kathleen Mills, & ASM International, eds. (2000). Metallography and Microstructures. [10. ed.], 9. print. Materials Park, Ohio: ASM International.

Berins, Michael L. (2012). SPI Plastics Engineering Handbook of the Society of the Plastics Industry, Inc. Springer Science & Business Media, Springer New York, NY.

Chen, K., & Hung-Mao, L. (2024). Effects of Niobium Carbide Additions on Ni-Based Superalloys: A Study on Microstructures and Cutting-Wear Characteristics through Plasma-Transferred-Arc-Assisted Deposition. *Coatings,* 14(2), 167. doi: 10.3390/coatings14020167.

Das, A. K., & Ravi, K. (2024). Investigation on Wear Behaviour of TiC/Co/Y2O3 Metal Matrix Composite Coating Developed on AZ91D Mg Alloy by Plasma Transferred Arc Cladding Process. *Materials Letters,* 355, 135457. doi: 10.1016/j.matlet.2023.135457.

Ferreira, L. S., Karin, G, Adriano, S., Luciano, S. F., Karin, G., & Adriano, S. (2015). Microstructure and Properties of Nickel-Based C276 Alloy Coatings by PTA on AISI 316L and API 5L X70 Steel Substrates. *Materials Research*, 18(1), 212–21. doi: 10.1590/1516-1439.332914.

Guo, X., Peng, Z., Hui, L., & Mengyu, W. (2023). Design and Performance of Nitrogen-Alloyed Iron-Based Coating for Enhancing Galling Resistance by Plasma Transferred Arc Welding. *Materials Letters*, 346, 134535. doi: 10.1016/j.matlet.2023.134535.

Hemmati, I., Rao, J. C., Ocelík, V., & Hosson, J. M. De. (2013). Electron Microscopy Characterization of Ni-Cr-B-Si-C Laser Deposited Coatings. *Microscopy and Microanalysis*, 19(1), 120–31. doi: 10.1017/S1431927612013839.

Hirpara, K. P., Janak, B. V., Mrunalkumar, D. C., & Milind, A. S. (2024). A Comprehensive Review on Recent Developments in Materials and Technological Parameters for Plasma Transferred Arc Hardfacing Process. *Proceedings of the Institution of Mechanical Engineers, Part E: Journal of Process Mechanical Engineering*, 238(3), 1507–19. doi: 10.1177/09544089231153363.

Kato, K. (2000). Wear in Relation to Friction — a Review. *Wear*, 241(2), 151–57. doi: 10.1016/S0043-1648(00)00382-3.

Kesavan, D., & Kamaraj, M. (2010). The Microstructure and High Temperature Wear Performance of a Nickel Base Hardfaced Coating. *Surface and Coatings Technology*, 204(24), 4034–43. doi: 10.1016/j.surfcoat.2010.05.022.

Kishore, K., Nikita, J., Anand, P., & Kanwer, S. A. (2023). Through-Thickness Microstructure and Wear Resistance of Plasma Transferred Arc Stellite 6 Cladding: Effect of Substrate. *CIRP Journal of Manufacturing Science and Technology*, 42, 24–35. doi: 10.1016/j.cirpj.2023.01.014.

Li, S., Xuanpu, D., Ali, C., Yutao, P., Xun, Z., Ying, C., Jeff, Th. M. H., & Huatang, C. (2023). In-Situ Micromechanical Analysis of a High-Vanadium High-Speed Steel Coating Made with Additive Manufacturing. *Materials Science and Engineering: A,* 870, 144850. doi: 10.1016/j.msea.2023.144850.

López, X. A., Muñoz-Arroyo, R., Hernández-García, F. A., Alvarez-Vera, M., Mtz-Enriquez, A. I., Díaz-Guillen, J. C., Isidro, G. F., Betancourt-Cantera, J. A., & Hdz-García, H. M. (2023). Processing of Co-Base/C-Nanotubes Compound Coatings on D2 Steel Using Plasma Transferred by Arc: Tribological and Mechanical Performance. *Surface and Coatings Technology*, 461, 129458. doi: 10.1016/j.surfcoat.2023.129458.

Lu, S., & Oh-Yang, K. (2002). Microstructure and Bonding Strength of WC Reinforced Ni-Base Alloy Brazed Composite Coating. *Surface and Coatings Technology*, 153(1), 40–48. doi: 10.1016/S0257-8972(01)01555-9.

Maros, M. B., & Shiraz, A. S. (2022). Tribological Study of Simply and Duplex-Coated CrN-X42Cr13 Tribosystems under Dry Sliding Wear and Progressive Loading Scratching. *Ceramics*, 5(4), 1084–1101. doi: 10.3390/ceramics5040077.

Mennig, G., & Klaus, S. (2013). Materials for Mold Making. Pp. 421–70 in Mold-making Handbook (Third Edition). Hanser.

Öteyaka, M. Ö., Arslan, A. E., & Çakir, F. H. (2021). Wear and Corrosion Characterisation of AISI 1030, AISI 1040 and AISI 1050 Steel Coated with Shielded Metal Arc Welding (SMAW) and Plasma Transfer Arc (PTA) Methods. *Sādhanā,* 46(3), 134. doi: 10.1007/s12046-021-01661-w.

Silva, L. J., & D'Oliveira, A. S. C. M. (2017). NiCrSiBC Alloy: Microstructure and Hardness of Coatings Processed by Arc and Laser. *Welding International*, 31(1), 1–8. doi: 10.1080/09507116.2016.1218608.

Sun, H., Sugui, T., Ning, T., Huichen, Y., & Xianlin, M. (2014). Microstructure Heterogeneity and Creep Damage of DZ125 Nickel-Based Superalloy. *Progress in Natural Science: Materials International*, 24(3), 266–73. doi: 10.1016/j.pnsc.2014.05.004.

Takaki, S., Tadashi, F., & Youichi, T. (1990). Effect of Si and Al Additions on the Low Temperature Toughness and Fracture Mode of Fe-27Mn Alloys. *ISIJ International*, 30(8), 632–38. doi: 10.2355/isijinternational.30.632.

Yang, G., Chao-peng, H., Wen-ming, S., Jian, L., Jin-jun, L., Ying, M., & Yuan, H. (2016). Microstructure Characteristics of Ni/WC Composite Cladding Coatings. *International Journal of Minerals, Metallurgy, and Materials*, 23(2), 184–92. doi: 10.1007/s12613-016-1226-z.

Zhou, Y., Rui, L., Heng, L., Yu, Y., Li, Z., Wuxi, Z., Wei, Y., & Chaofang, D. (2023). Influence of Tungsten Carbide Raw Materials to Microstructure and Wear Performance on PTA Hard-Facing Materials with Its Micro-Mechanism Analysis. *Surface and Coatings Technology*, 454, 129200. doi: 10.1016/j.surfcoat.2022.129200.